

Study of optical properties of highly oriented nanocrystalline $V_2O_5 \cdot nH_2O$ films doped with K ions

Hoda A. Mady · Samia E. Negm ·
A. S. Abdel Moghny · A. S. Abd-Rabo ·
A. A. Bahgat

Received: 21 May 2011 / Accepted: 1 January 2012 / Published online: 20 January 2012
© The Author(s) 2012. This article is published with open access at Springerlink.com

Abstract Optical transmission and reflection measurements of highly oriented nanocrystalline $K_xV_2O_5 \cdot nH_2O$ films ($0 \leq x < 0.01$) were studied. The optical constants such as, refractive index, the extinction coefficient, absorption coefficient, optical band gap have been calculated. The optical spectra of all samples exhibited two distinct regions of optical gap, E_{op1} suggesting a direct allowed transition with optical gap ranging from 0.37 up to 0.42 eV and E_{op2} suggesting a direct forbidden transition with optical gap ranging from 2.02 up to 2.23 eV. This indicates that $K_xV_2O_5 \cdot nH_2O$ films have more than one type of conduction mechanism.

Keywords Sol–gel · Vanadium pentoxide · Optical properties · Conduction mechanisms

1 Introduction

The sol–gel procedure is a suitable synthetic path for creating materials with very different properties as compared to usual solid-state chemical techniques; on the other hand it offers a low cost approach for the production of electrochromic films [1]. It was found that the low temperature products have lower crystallinity and higher specific capacity than those synthesized by high temperature solid state method [2]. The wide variety of technological applications of $V_2O_5 \cdot nH_2O$ xerogel such as chemical sensors,

optical memory switching and optical fibers give rise to its scientific interest [3–5]. Electronic transport is observed by electron hopping mechanism in materials containing transition metal ions such as Fe, Co, V, etc. if these ions are present in two distinct oxidation states via electrons hopping along e.g. V^{4+} -O- V^{5+} paths [6]. The optical properties of highly oriented nanocrystalline hydrated vanadium pentoxide, $V_2O_5 \cdot nH_2O$, prepared by dissolving V_2O_5 powder in hydrogen peroxide, H_2O_2 solution revealed that two different optical gaps are present, $E_{op1} = 0.37$ eV and $E_{op2} = 2.2$ eV, respectively [7]. Generally, the fundamental electronic structure of the present system is formed by the oxygen O-2*p* and vanadium V-3*d* orbitals [8]. The oxygen 2*p* states have the lowest energy (the highest binding energy). They form a band of 4.0 eV wide, which is fully occupied. The occupied part of the V-3*d* states is positioned about 3.0 eV above the top of the oxygen bands. Due to field splitting the V-3*d* manifold is spread over a range of at least 3 eV. The 3*d*_{xy} level of the V^{4+} is occupied with one electron. The unoccupied *d*_{xz} and *d*_{yz} levels are at least 1.0 eV higher. These in turn are located about 2 eV below *d*_{x²-y²} and the *d*_{z²} levels. The relevance of the O-2*p* bands is that they provide a path for virtual hopping process between the V sites. The coupling between V sites is through virtual hopping via π -bonded O-2*p*_y states [9]. These observations are consistent with the fact that these absorption bands are electronic *d*-*d* transitions associated with V^{4+} centers in a low-symmetry crystal field environment with square pyramidal C_{2v} symmetry [10].

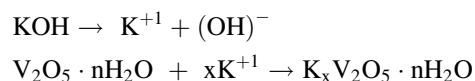
In the present study optical transmittance and reflectance were investigated for $K_xV_2O_5 \cdot nH_2O$ films, where ($0 \leq x < 0.01$). Investigation of the spectral distribution of the refractive index, *n*, the extinction coefficient, *k*, and hence the absorption coefficient, α , were made. An analysis of the absorption coefficient has been carried out to obtain the

H. A. Mady · S. E. Negm · A. S. A. Moghny ·
A. S. Abd-Rabo · A. A. Bahgat (✉)
Department of Physics, Faculty of Science, Al-Azhar University,
Nasr City, Cairo 11884, Egypt
e-mail: alaabahgat@yahoo.com

optical band gap, E_g^{Opt} , the band tail width, E_c , and the nature of transitions mechanism involved as well.

2 Experimental techniques

Five different compositions of $K_xV_2O_5 \cdot nH_2O$ (where $x = 0.00, 0.0017, 0.0049, 0.0064$ and 0.0091 mol) have been prepared for the present investigation. Films of the investigated compounds were prepared by sol–gel technique (colloidal route) [11]. The powder of vanadium pentoxide (V_2O_5) (99.99%) and potassium hydroxide (KOH) (99.99%) in suitable proportions (mol %) were used as raw materials. A batch of (1.04 g) of V_2O_5 was dissolved in 80 mL of 17.5% hydrogen peroxide (H_2O_2) at room temperature [6]. The formed solution was stirred continuously using magnetic stirrer. The solution was then heated at 60 °C, with uninterrupted continuous stirring, while pH was 3–4. Water dissolved KOH (0.07 mol) was added to the V_2O_5 gel drop by drop using a Pruitt up to the desired concentration according to the following chemical reaction



Vanadium pentoxide (V_2O_5) and (V_2O_5 -(x) KOH) gels can be synthesized via the condensation of aqueous solutions of (V_2O_5) and (V_2O_5 -(x) KOH). The obtained gels without precipitation are limited to the range of x recorded is due to the KOH chemical alkalinity effect which increases the pH value above the suitable acidic requirements. No surfactant was used during preparation of the films which were obtained by the deep coating of Pyrex substrate (microscope glass slide). The films thickness were measured using optical interference technique using type ZYGO-Maxim Interferometer microscope, the obtained results are given in Table 1. Film’s properties are determined by calculating reflectance and transmittance as a function of wavelength based on the values of the thickness and the n and k parameters. To measure the transmission and the reflection of the films under test, JASCO V-570 spectrophotometer, SP, was used. The SP is a double beam instrument consisting of a double monochromator of grating type. The SP is linked to a PC for data acquisition. Slit width or signal amplification gain

Table 1 Film thicknesses-for the system $K_xV_2O_5 \cdot nH_2O$

x (mol)	Thickness (nm)
0.0000	250
0.0017	190
0.0049	140
0.0064	300
0.0091	320

is also controlled automatically to adjust the base line before any series of measurements. Its spectral range extends from 190 nm in ultraviolet to 2,500 nm near infra red range. A clean Pyrex substrate of the type used to hold up the films was attached to the reference slit of the SP.

3 Results and discussion

3.1 Dispersion curves of refractive index and extinction coefficient

Recently the nanocrystalline structure [11] as well as the transport properties [12] of a series of $K_xV_2O_5 \cdot nH_2O$ films, where ($0 \leq x \leq 0.0091$) were investigated. Current results indicated that all films are composed of highly oriented nanocrystalline rod-like shape of size ranging from 9.7 to 14.7 nm as reported recently by us in Ref. [11]. On the other hand the electrical transport properties indicate a non-adiabatic small polaron hopping conduction mechanism this together with that the system is n-type semiconductor within the temperature range investigated [12].

The optical spectral distribution curves of transmittance, $T(\lambda)$, and reflectance, $R(\lambda)$, for $K_xV_2O_5 \cdot nH_2O$ films with $0.0 \leq x < 0.01$ shown in Fig. 1 have been used to compute the refractive index, n , and extinction coefficient, k , according to the following equations [13]:

$$R = \frac{(n - 1)^2 + k^2}{(n + 1)^2 + k^2} \tag{1}$$

If $k \ll n$ we may put;

$$n = \frac{1 + \sqrt{R}}{1 - \sqrt{R}} \tag{2}$$

While the absorption coefficient α for the films under test was calculated using the following equation [13]:

$$\alpha = \frac{1}{d} \ln \left(\frac{100 - R}{T} \right) \tag{3}$$

where d is the film thickness. And the extinction coefficient is obtained by;

$$k = \frac{\alpha \lambda}{4\pi} \tag{4}$$

Figure 2a and b show the obtained results where there was no significant difference between the forms of the curves for these films. While, n , follows the usual trend of increasing as the wave length of the incident photons decreases [14].

3.2 Spectral distribution of the absorption coefficient α

In many amorphous materials the absorption edge at higher energy range [$\alpha > 10^4 \text{ cm}^{-1}$] obeys Tauc’s law [13–15]:

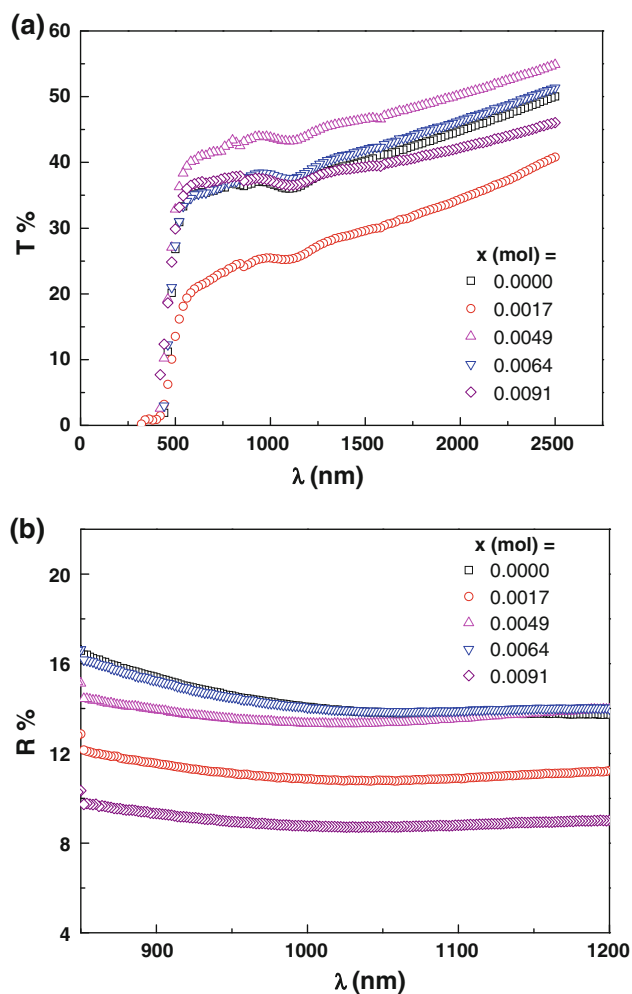


Fig. 1 Spectral distribution of **a** transmittance (T) and **b** reflectance (R) for $K_xV_2O_5 \cdot nH_2O$ films with $0.0 \leq x \leq 0.0091$

$$\alpha h\nu = \beta(h\nu - E_{op})^r \quad (5)$$

where β is constant called band tailing parameter, $h\nu$ is the incident photon energy and E_{opt} is the optical band gap energy. The exponent $r = 1/2$ or $3/2$ are for direct transition depends on whether the transition is allowed or forbidden, and $r = 2$ or 3 for allowed and forbidden indirect transitions, respectively. In order to distinguish between those different exponents one have to know first the value of E_{op} . This situation may be surmounted by the prior knowledge of the imaginary part of the dielectric permittivity, ε_2 , as a function of photon energy and which is recognized as the absorption spectrum [16].

The actual value of the optical gap for the investigated films can be established by studying the absorption band profile. The absorption is best given by a plot of the complex dielectric permittivity, $\varepsilon^* = \varepsilon_1 - i\varepsilon_2$ as a function of the incident energy, $h\nu$, where generally, $\varepsilon_1 = n^2 - k^2$ and $\varepsilon_2 = 2nk$. When the value of ε_2 is plotted as a function of energy in eV, the fundamental absorption spectrum is

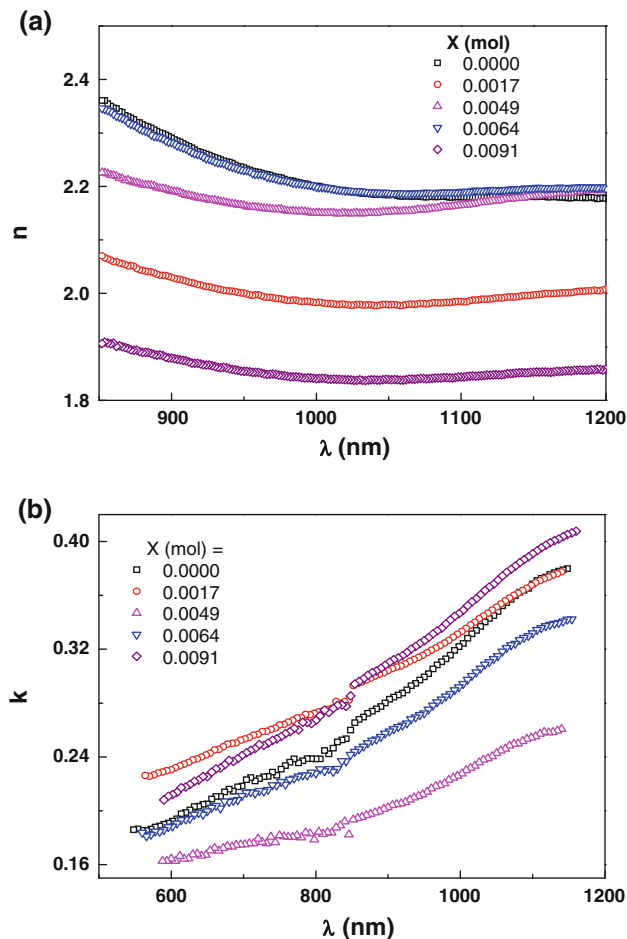


Fig. 2 Spectral dependence of **a** the refractive index (n) and **b** the extinction coefficient (k) for $K_xV_2O_5 \cdot nH_2O$ films with $0.0 \leq x \leq 0.0091$

obtained [16]. When the onset of the absorption spectrum (ε_2 vs. $h\nu$) is determined then, the value of the optical gap is obtained accordingly. Figure 3 shows the calculated values of ε_2 as a function of, $E = h\nu$, in eV for $K_xV_2O_5 \cdot nH_2O$ (with $0.00 \leq x \leq 0.0091$) system. In Fig. 3 it is observed that there are two independent absorption edges, indicating two different optical gaps [14]. The first edge if extrapolated to intersect with the E-axes produces the actual value of the optical gap, E_{op1} , while the second edge if extrapolated as well will bring the second actual optical gap, E_{op2} , as shown in Fig. 3. Accordingly the two different absorption edges are at ($E_{op1} = 0.37\text{--}0.41$ eV) and ($E_{op2} = 2.02\text{--}2.23$ eV) depending on different concentration of K-ions, respectively.

As the optical gaps were determined the usual procedure for determining the value of, r , is by applying Eq. 5 which involves plotting a graph of $(\alpha h\nu)^{1/r}$ against $h\nu$ as shown in Fig. 4a and b [13–15]. The optical band gap can be determined by extrapolation of the linear parts of the obtained curves as shown in Fig. 4a and b, while β can be

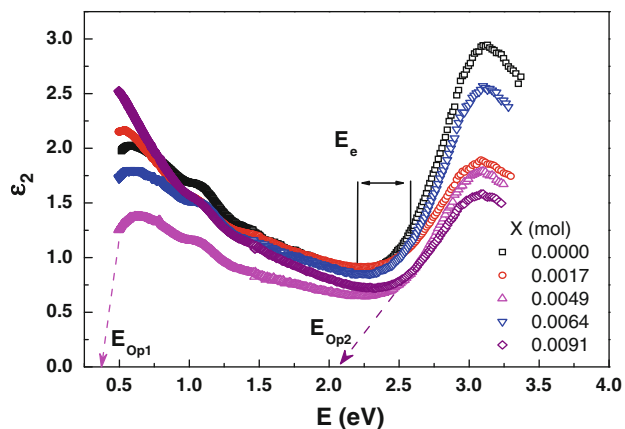


Fig. 3 The imaginary part of the dielectric constant ϵ_2 as a function of photon energy ($h\nu$) for $K_xV_2O_5 \cdot nH_2O$ for K different content

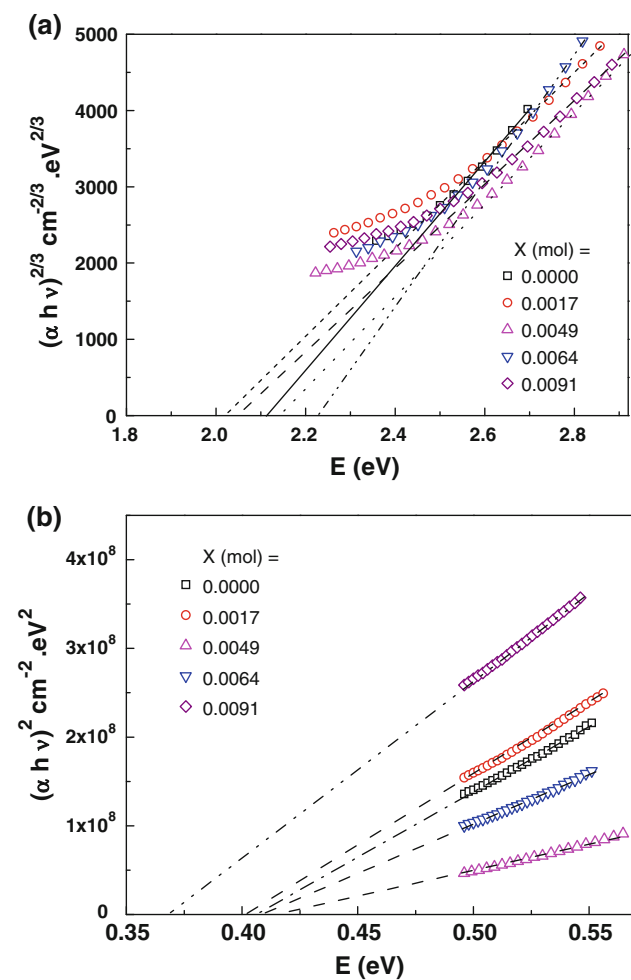


Fig. 4 Optical gaps as produced by extrapolating the linear parts of the absorption edge according to Eq. 5. **a** E_{Opt2} with the exponent $r = 3/2$, **b** E_{Opt1} with the exponent $r = 1/2$ for $K_xV_2O_5 \cdot nH_2O$ films with different K content

calculated on the other hand from the slope of the linear parts of the curves [13–15]. It is clearly found that the obtained optical gap changes with changing the value of

the exponent, r , as presented for example in Tables 2 and 3. The obtained linear regression coefficient doesn't as well facilitate a good indication of the value of r , which may be considered. To avoid this uncertainty one should apply the values of the optical gaps introduced from the absorption spectrum, (ϵ_2 vs. $h\nu$), of Fig. 3 explained above. This indicates that $K_xV_2O_5 \cdot nH_2O$ films have more than one type of conduction mechanism. The linear fitting to the data at the band edge and intersecting with the $h\nu$ axis at the same energy which is coincide with those obtained from the absorption spectrum, will give the value of r as well as the optical gap as shown in Fig. 4a and b.

Applying the results obtained from the absorption band (ϵ_2 vs. E of Fig. 3), it is noted that the first high energy band gives, E_{Opt2} , is in the range 2.02–2.27 eV as given in Table 4. This gap is characterized by a direct forbidden transition with $r = 3/2$, see Fig. 4a. The result for $V_2O_5 \cdot nH_2O$ sample is in good agreement with results that obtained in [17]. These results can be compared with those obtained for sputtered

Table 2 Representation of the obtained values of the optical gap E_{Opt1} at different values of the exponent r for $K_xV_2O_5 \cdot nH_2O$ system with $0 \leq x < 0.01$

$K_{0.0017}V_2O_5 \cdot nH_2O$			E_{Opt1} (eV)
Type of transition	r	E_{opt1} (eV)	Calculated from absorption band ϵ_2
Indirect allowed	2	-0.07	0.41
Indirect forbidden	3	-0.31	
Direct forbidden	3/2	0.09	
Direct allowed	1/2	0.42	

Table 3 Representation of the obtained values of the optical gap E_{Opt2} at different values of the exponent r for $K_xV_2O_5 \cdot nH_2O$ system with $0 \leq x < 0.01$

$K_{0.0017}V_2O_5 \cdot nH_2O$			E_{Opt2} (eV)
Type of transition	r	E_{opt2} (eV)	Calculated from absorption band ϵ_2
Indirect allowed	2	1.8	2.02
Indirect forbidden	3	1.3	
Direct forbidden	3/2	2.02	
Direct allowed	1/2	2.61	

Table 4 Optical parameters as calculated, E_{Opt} is the optical gap, E_e is band tail width

x (mol)	E_{Opt1} (eV)	$E_{Opt 2}$ (eV) $r = 3/2$	E_{Opt2} (eV) from ϵ_2	β ($\times 10^4$ cm $^{-1}$ eV $^{-1/2}$)	E_e (eV)
0.0000	0.406	2.17	2.27	0.684	0.50
0.0017	0.402	2.02	2.02	0.590	0.66
0.0049	0.420	2.11	2.17	0.619	0.58
0.0064	0.401	2.23	2.23	0.858	0.45
0.0091	0.370	2.09	2.06	0.575	0.80

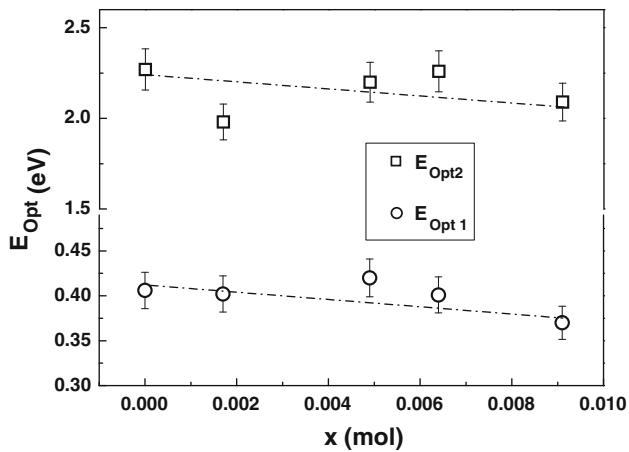


Fig. 5 The obtained results for E_{Opt1} and E_{Opt2} as a function of composition $K_xV_2O_5 \cdot nH_2O$ with $0 \leq x \leq 0.0091$

V_2O_5 thin films in [18] and other works [19–22]. Furthermore, the second region for $h\nu < 0.6$ eV is best presented by an absorption band with a gap of E_{Opt1} around 0.4 eV and $r = 1/2$, see Fig. 4b. This low energy absorption is associated with the intra band transitions involving deep impurity states within the energy gap and/or to a second gap in the phase space of lower energy and is described by a direct allowed transition. Figure 5 shows the obtained results for E_{Opt1} and E_{Opt2} as a function of composition of $K_xV_2O_5 \cdot nH_2O$ with $0.00 \leq x < 0.01$.

Apparently, it should be noted that any variation in the band gap might be associated with the level of ordering in $K_xV_2O_5 \cdot nH_2O$ films. Where when, $r = 3/2$, in a direct transition no phonons are created or adsorbed during the transition itself. Therefore, this may be true in amorphous or glassy materials where phonons concept is due to the ordered structure of crystalline solids. Additionally, if one compare the electrical conductivity results from Ref. [12] and the present optical gap, it is clear that $E_{Opt1} = 2W_{dc}$; here W_{dc} is the activation energy of electronic conduction; indicating an intrinsic like semiconducting state. Moreover, from plotting $\ln \alpha$ as a function of, $h\nu$, as shown in Fig. 6, values of, E_c ; (known as the Urbach tail and which is the band tail width); as a function of composition can be calculated and given in Table 4, where generally [13, 15];

$$\alpha = \alpha_0 \exp(h\nu/E_c) \quad (6)$$

E_c representing the exponential band tail which may take place from static spatial fluctuations in potential arising from the lack of long range order or charged defects centers [16].

3.3 Determination of carrier concentration and the electron effective mass

The obtained data of refractive index n can be further analyzed to obtain the high frequency dielectric constant

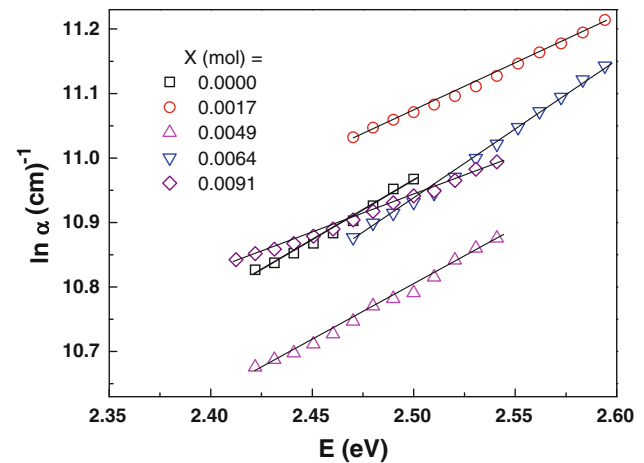


Fig. 6 Plots of $\ln \alpha$ as a function of photon energy ($h\nu$) for films of different K content

ϵ_∞ according to the following procedure [7]. This procedure is describing the contribution of the free carriers and the lattice vibrational modes of the dispersion. According to Pankove [13]:

$$\epsilon_1 = \epsilon_\infty - \frac{e^2 N_t}{\pi \epsilon_0 m^* c^2} \lambda^2 \quad (7)$$

where ϵ_1 is the real part of the dielectric constant, ϵ_∞ is the lattice dielectric constant, λ is the wavelength, e is the electronic charge, N_t is the free-charge carrier concentration, ϵ_0 is the permittivity of the free space, m^* is the effective mass of charge carriers, c is the velocity of light.

It is observed that the dependence of ϵ_1 on λ^2 is linear at longer wavelengths, as shown in Fig. 7. Extrapolating the linear part to intersect the Y axis will give the values of ϵ_∞ and from the slopes of these lines we can calculate the values of N/m^* for the investigated films. Values of ϵ_∞ and N/m^* are given in Table 5. Applying the previously

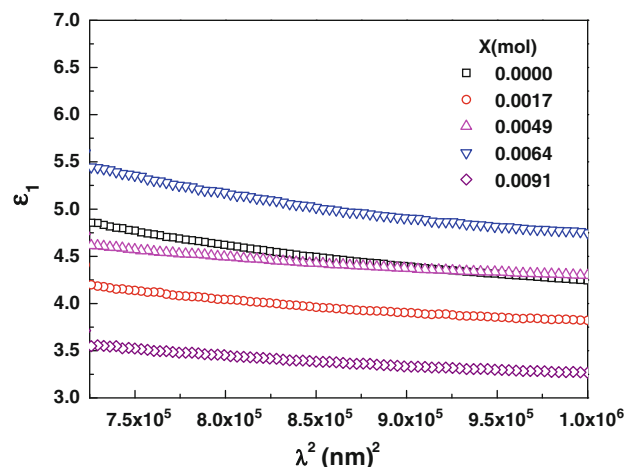


Fig. 7 Real part of the dielectric constant as a function of λ^2 for different compositions $K_xV_2O_5 \cdot nH_2O$ with $0 \leq x \leq 0.0091$

Table 5 The obtained results of charge carrier concentration and effective mass of the present system

x (mol)	ϵ_∞	N/m^* ($10^{27} \text{ m}^{-3} \text{ kg}^{-1}$)	N_t $\times 10^{27} \text{ m}^{-3}$ Ref. [11]	m^*/m
0.0000	4.50	15.229	7.676	0.553
0.0017	4.46	17.428	7.680	0.484
0.0049	5.24	18.760	7.700	0.451
0.0064	5.82	19.651	7.701	0.430
0.0091	4.51	19.959	7.730	0.425

reported values of the xerogel films carrier concentration, N_t , [12] it is possible to calculate the charge carriers effective mass relative to the free electron rest mass, m_e , as presented in Table 5. The obtained values of the optical relative dielectric permittivity $\epsilon_\infty = n_o^2$ are of the same order with those obtained by Chopra et al. [15] for $\text{V}_2\text{O}_5\text{-TeO}_2$ films as well as for xerogel system of the composition $\text{Li}_x\text{V}_2\text{O}_5 \cdot n\text{H}_2\text{O}$ [23].

4 Conclusions

In the present work, highly orientated nanocrystalline films with excellent properties can be prepared by sol–gel technique, where:

- (1) Optical measurements revealed that two optical gaps are present.
- (2) E_{Op1} with exponent $r = 1/2$ suggesting a direct allowed transition with an evaluated optical gap from 0.37 to 0.42 eV.
- (3) E_{Op2} with exponent $r = 3/2$ suggesting a direct forbidden transition with an evaluated optical gap from 2.02 to 2.23 eV.
- (4) The width of the localized states (band tail) E_c were estimated from the slopes of $\ln \alpha$ & $h\nu$ plots of the samples and have values in the range 0.45–0.80 eV.
- (5) Electronic effective masses have been calculated in the range 0.42–0.55 m_e , indicating a relatively light Fermions.

Open Access This article is distributed under the terms of the Creative Commons Attribution Noncommercial License which permits any noncommercial use, distribution, and reproduction in any medium, provided the original author(s) and source are credited.

References

1. Ozer N, Lampert CM (1996) Solar Energy Mater solar cells 54(1):147
2. Xie J, Li J, Zhan H, Zhou Y (2003) Mater Lett 57:2682
3. Montani RA, Levy M, Souquent JL (1992) J Non Cryst Solids 149:249
4. Ghosh A, Chaudhri BK (1988) J Non Cryst Solids 103:83
5. Bahgat AA, Ibrahim FA, El-Desoky MM (2011) AIP Conf Proc 1370:61
6. Linsley GS, Owen AE, Hayatee FM (1970) J Non Cryst Solids 4:208
7. Bahgat AA, Ibrahim FA, El-Desoky MM (2005) Thin Solid Films 489:68
8. Khyzhun OYU, Strunskus T, Grunent W, Wöll Ch (2005) J Electron Spectrosc Relat Phenom 149(1–3):45
9. Liu YJ, Cowen JA, Kaplan TA, Degroot DC, Schindler J, Kannewurf CR, Kanatzidis MG (1995) Chem Mater 7:1616
10. Yao T, Oka Y, Yamamoto N (1992) Mat Res Bull 27:669
11. Negm SE, Mady HA, Abdel Moghny A, Abd-Rabo AS, Bahgat AA (2011) Solid State Sci 13:590
12. Bahgat AA, Mady HA, Abdel Moghny AS, Abd-Rabo AS, Negm SE (2011) J Mater Sci Technol 27(10):865
13. Pankove JI (1971) Optical processes in semiconductors. Engle Wood Cliffs
14. Bahgat AA, Abd Rabo AS, Mahdy IA, Mahmoud EA (2008) Opt Laser Technol 40:1061
15. Chopra KL (1969) Thin film phenomena. McGraw-Hill, New York
16. Mott NF, Davis EA (1979) Electronic process in non-crystalline materials. Clarendon Press, Oxford
17. Benmoussa M, Outzourhit A, Jourdani R, Bennouna A, Amezi-ane EL (2003) Act Passiv Elec Comp 26(4):245
18. Benmoussa M, Ibnouelghazi E, Bennouna A, Amezi-ane EL (1995) Thin Solid Films 265:22
19. Ozer N (1997) Thin Solid Films 305:80
20. Rubin M, Van Rottkay K, Wen SJ, Ozer N, Slack J (1998) Solar Energy Mater Solar Cells 54:49
21. Madhuri KV, Naidu BS, Hussain OM, Eddrief M, Julien C (2001) Mater Sci Eng B 86:165
22. Ramana CV, Hussain OM, Srinivasulu B, Julien C, Balkanski M (1998) Mater Sci Eng B 52:32
23. Al-Assiri MS, El-Desoky MM, Alyamani A, Al-Hajry A, Al-Mogeeth A, Bahgat AA (2010) Opt Laser Technol 42:994